Journal of Vibration and Control
http://jvc.sagepub.com/

Vibration suppression of curved beam-type structures using optimal multiple tuned mass dampers

F Yang, R Sedaghati and E Esmailzadeh

Journal of Vibration and Control 2014 20: 859 originally published online 12 December 2012
DOI: 10.1177/1077546312468461

Article

Journal of Vibration and Control
2014, Vol. 20(6) 859–875

DOI: 10.1177/1077546312468461
jvc.sagepub.com
SAGE

Vibration suppression of curved beam-type structures using optimal multiple tuned mass dampers

F Yang[1], R Sedaghati[2] and E Esmailzadeh[3]

Abstract

This paper established a thorough optimization procedure of the multiple tuned-mass-damper system to suppress the vibration levels of the curved beam-type structures with multiple vibration dominant modes. A hybrid optimization methodology, which combines the global optimization method based on the Genetic Algorithm and the local optimization method based on Sequential Quadratic Programming, has been developed. The established hybrid optimization procedure is then utilized to find the optimum values of the design parameters, namely, the spring stiffness, damping factor and the position of the attached tuned-mass-damper systems, in order to suppress the vibration amplitude either at a particular mode or at several modes simultaneously.

Keywords

Curved beam, random loading, tuned-mass-dampers, hybrid optimization, Genetic Algorithm, Sequential Quadratic Programming

Received: 24 August 2012; revised: 9 October 2012

1. Introduction

The tuned-mass-damper (TMD) technique is one of the most applicable passive vibration suppression technologies. Previous research papers about the TMD design are mainly related to attaching a single or multiple TMDs onto (1) the Single-Degree-of-Freedom (SDOF) main structure, such as the research work presented by Den Hartog (1956), Igusa and Xu (1994), Rana and Soong (1998) and Rüdinger (2006); (2) the discrete Multi-Degree-of-Freedom (MDOF) main structure, such as the building-type structures (Rana and Soong, 1998); (3) the continuous systems with a single distinct dominant vibration mode, and a known location of the TMD or MTMD (Chen and Huang, 2004; Younesian et al., 2006).

An important issue related to the design of TMD(s) for continuous structures is the location of the attached TMD(s). Based on the working principle of an optimally designed TMD system, Fitzpatrick stated that the "TMD(s) are close to the antinodes of the modes as they are considered as damping" (Fitzpatrick et al., 2001). However, it should be noted that "close" is quite a vague definition for the optimal TMD system. To obtain the best vibration suppression performance, especially for the main continuous structures with multiple dominant vibration modes or antinodes, it is necessary to establish an optimal procedure to evaluate the optimum values of the location, numbers and parameters of the TMD system efficiently, and/or to verify the validity of directly installing the TMD at the close position of each antinode. The above issues are the main objectives of this study.

Although the position of TMDs has been expressed as a variable in the established equations of motion in

[1]College of Automation Science and Engineering, South China University of Technology, P.R. China
[2]Department of Mechanical and Industrial Engineering, Concordia University, Canada
[3]Faculty of Engineering and Applied Science, University of Ontario Institute of Technology, Canada

Corresponding author:
Ebrahim Esmailzadeh, University of Ontario Institute of Technology, 2000 Simcoe Street North, Oshawa, ON, Canada L1H 7K4.
Email: ezadeh@uoit.ca

the research works presented by Manikanahally and Crocker (1991), Rice (1993) and Esmailzadeh and Jalili (1998), it has been assumed as a given input in the design optimization procedure. Recently, Yang et al. (2009, 2010) established and verified the validity of a Finite Element (FE) approach to investigate the TMD design problem for vibration suppression of beam-type structures (Timoshenko and curved beams). However, those articles (Yang et al., 2009, 2010) are focused on the attachment of a single TMD at a specific position along the beams.

In this study, the location of the TMD system will be considered as one of the design variables, which is one of the essential issues of the application of TMD in structures. A general form of curved beams with multiple dominant vibration modes is utilized to investigate the MTMD design for continuous structures. The curved beam is modeled, including the radial and tangential displacement, and rotation deformation. The governing equations of motion will be solved using the FE approach developed by Yang et al. (2008). The FE approach of the combined curved beam with the TMD system will be developed in this study based on the work published by Yang et al. (2009, 2010).

Since the location of the TMD system is considered as one of the design variables, the established optimization problem would not be a simple local case. Therefore, a hybrid optimization method that combines the global optimization technique, based on the Genetic Algorithm (GA) (Haupt and Haupt, 2004), with the local optimization method using Sequential Quadratic Programming (SQP) (Rao, 1996), has been developed. The established hybrid optimization method was then utilized to attain the optimum values of the design parameters, namely, spring stiffness, damping factor and the attachment position of the TMD systems. Illustrated examples have been considered to verify the validity of the developed MTMD design methodology.

2. Curved beams with attached multiple tuned mass dampers

A general curved beam with the attached MTMD system has been illustrated in Figure 1. The parameters L, Φ, h and s represent the span length, curve angle, rise and curvilinear coordinate of the curved beam, respectively. The variables $y(x)$ and $\rho(s)$ are the respective functions describing the center line and the radius of the curved beam. Parameters S_{Ti}, K_{TMDi}, C_{TMDi} and M_{TMDi} are the position along the s coordinate, stiffness, viscous damping and the mass of the ith attached TMDs, respectively, which are all considered as the design variables in this study.

The formulations presented here are based on the curved beam model, with the consideration of the axial extensity, shear deformation and the rotary inertia (Yang et al., 2008), with two TMDs. The expressions of kinetic energy (T), potential energy (V) and the non-conservative virtual work (δW_{nc}) can be described as

$$
\begin{aligned}
T = & \frac{1}{2}\int_L m(s)\left(\frac{\partial w(s,t)}{\partial t}\right)^2 ds + \frac{1}{2}\int_L J(s)\left(\frac{\partial \psi(s,t)}{\partial t}\right) ds \\
& + \frac{1}{2}\int_L m(s)\left(\frac{\partial u(s,t)}{\partial t}\right)^2 + \frac{1}{2} M_{TMD1}\bar{Z}_{T1}(t)^2 \\
& + \frac{1}{2_{TMD2}}\bar{Z}_{T2}(t)^2
\end{aligned}
\tag{1a}
$$

$$
\begin{aligned}
V = & \frac{1}{2}\int_L EI(s)\left(\frac{\partial \psi(s,t)}{\partial s}\right)^2 ds + \frac{1}{2}\int_L k_q GA(s)\beta^2(s,t) ds \\
& + \frac{1}{2}\int_L EA(s)\left(\frac{\partial u_T(s,t)}{\partial s}\right)^2 ds + \frac{1}{2}K_{TMD\,1}[w(s_{T1},t)\cos(\alpha_{s_{T1}}) \\
& + u(s_{T1},t)\sin(\alpha_{s_{T1}}) - z_{T1}(t)]^2 + \frac{1}{2}K_{TMD\,2}[w(s_{T2},t)\cos(\alpha_{s_{T2}}) \\
& + u(s_{T2},t)\sin(\alpha_{s_{T2}}) - z_{T1}(t)]^2
\end{aligned}
\tag{1b}
$$

$$
\begin{aligned}
\delta W_{nc} = & \int_L f(s,t)\delta w ds + \int_L -C_w \dot{w}(s,t)\delta w ds \\
& + \int_L -C_u \dot{u}(s,t)\delta u ds - C_{TMD1}[\dot{w}(s_{T1},t)\cos(\alpha_{s_{T1}}) \\
& + \dot{u}(s_{T1},t)\sin(\alpha_{s_{T1}}) - \dot{z}_{T1}(t)] \times \delta[w(s_{T1},t)\cos(\alpha_{s_{T1}}) \\
& + u(s_{T1},t)\sin(\alpha_{s_{T1}}) - z_{T1}(t)] - C_{TMD2}[\dot{w}(s_{T2},t)\cos(\alpha_{s_{T2}}) \\
& + \dot{u}(s_{T2},t)\sin(\alpha_{s_{T2}}) - \dot{z}_{T2}(t) \times \delta[w(s_{T2},t)\cos(\alpha_{s_{T2}}) \\
& + u(s_{T2},t)\sin(\alpha_{s_{T2}}) - z_{T2}(t)]
\end{aligned}
\tag{1c}
$$

where $w(s)$, $u(s)$, $w(s)/\rho(s)$ and $u_T(s)$ are the respective transverse displacement, tangential displacement, the tangential displacement due to the radial displacement and the total tangential displacement of the beam.

The variables $\psi(s)$, $\beta(s)$ and $dw(s)/ds$ are the rotation due to bending, rotation due to shear deformation and slope of radial deflection (w) curve, respectively, and $du_T(s)/ds = du(s)/ds + w(s)/\rho(s)$; $dw(s)/ds = \beta(s) + \psi(s) + u(s)/\rho(s)$ (Yang et al., 2008). The variables $m(s)$, $A(s)$, $I(s)$ and $J(s)$ represent the linear density, cross-sectional area, and the area and mass moments of inertia, respectively.

The parameters E, G, k_q, C_w and C_u are the modulus of elasticity, shear modulus, sectional shear coefficient and the viscous damping coefficients along the radial and tangential directions of the curved beam, respectively. Variables $\alpha_{S_{T1}}$ and $\alpha_{S_{T2}}$ represent the angle between the curved beam's center line tangential direction and the X-axis at the location of the attached first

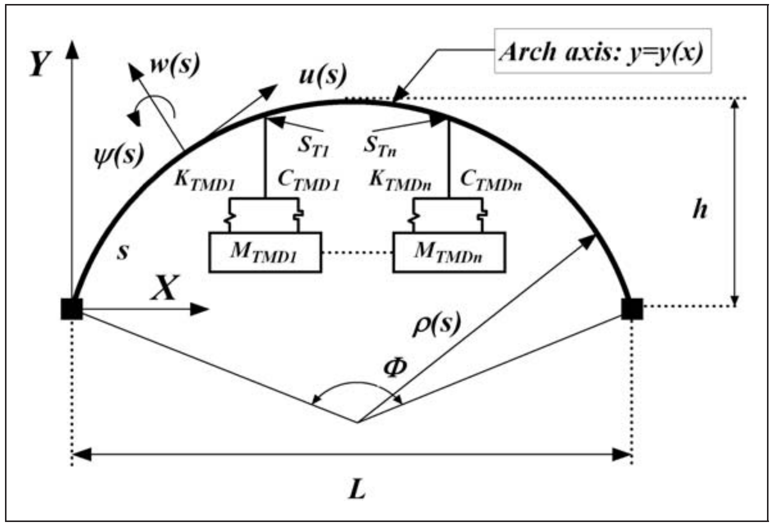

Figure 1. General curved beam with the attached multiple tuned-mass-damper system.

and second TMDs, respectively. The variables $w(s_{T1},t)$ and $u(s_{T1},t)$ are the respective radial and tangential displacements of the beam at the position of the first attached TMD, and $w(s_{T2},t)$ and $u(s_{T2},t)$ are those for that of the position of the second attached TMD. The parameters z_1 and z_2 represent the respective displacements of the first and second attached TMDs. The integral symbol, $\int_L [.]ds$, is the curvilinear integral taken along the s coordinate, and $f(s,t)$ is the external force.

The governing differential equations of motion for the design problem shown in Figure 1 can be obtained by applying the Hamilton principle to Equation (1). Based on the methodology developed by Yang et al. (2009, 2010), the TMD system can be enrolled in the differential equations of motion. Then to relate the variables $x(s)$, $y(s)$, the radial displacement $w(s)$, tangential displacement $u(s)$, rotation due to the bending $\psi(s)$, cross-section area $A(s)$, and the area moment of inertia $I(s)$ to their nodal values through the Lagrangian type shape functions (Yang et al., 2008), one can discretize the established differential equations of motion to obtain the following governing equations of motion in the FE form as

$$M\ddot{\mathbf{q}}(t) + C\dot{\mathbf{q}}(t) + \mathbf{K}\mathbf{q}(t) = \mathbf{F}(t) \tag{2}$$

where

$$\mathbf{q} = \left\{ \mathbf{w}(t) \quad \mathbf{u}(t) \quad \psi(t) \quad z_T1(t) \quad z_T2(t) \right\}^{\mathrm{T}} \tag{3a}$$

$$\mathbf{M} = \begin{bmatrix} \mathbf{M}_{ww} & \mathbf{0} & \mathbf{0} & \mathbf{0} & \mathbf{0} \\ \mathbf{0} & \mathbf{M}_{uu} & \mathbf{0} & \mathbf{0} & \mathbf{0} \\ \mathbf{0} & \mathbf{0} & \mathbf{M}_{\psi\psi} & \mathbf{0} & \mathbf{0} \\ \mathbf{0} & \mathbf{0} & \mathbf{0} & M_{TMD1} & 0 \\ \mathbf{0} & \mathbf{0} & \mathbf{0} & 0 & M_{TMD2} \end{bmatrix} \tag{3b}$$

$$\mathbf{K} = \begin{bmatrix} \mathbf{K}_{ww} + \mathbf{K}_{wwT1} + \mathbf{K}_{wwT2} & \mathbf{K}_{wu} + \mathbf{K}_{wuT1} + \mathbf{K}_{wuT2} & \mathbf{K}_{w\psi} & \mathbf{K}_{wz1} & \mathbf{K}_{wz2} \\ \mathbf{K}_{wu}^{\mathrm{T}} + \mathbf{K}_{wuT1}^{\mathrm{T}} + \mathbf{K}_{wuT2}^{\mathrm{T}} & \mathbf{K}_{uu} + \mathbf{K}_{uuT1} + \mathbf{K}_{uuT2} & \mathbf{K}_{u\psi} & \mathbf{K}_{uz1} & \mathbf{K}_{uz2} \\ \mathbf{K}_{w\psi}^{\mathrm{T}} & \mathbf{K}_{u\psi}^{\mathrm{T}} & \mathbf{K}_{\psi\psi} & \mathbf{0} & \mathbf{0} \\ \mathbf{K}_{wz1}^{\mathrm{T}} & \mathbf{K}_{uz1}^{\mathrm{T}} & \mathbf{0} & K_{TMD1} & 0 \\ \mathbf{K}_{wz2}^{\mathrm{T}} & \mathbf{K}_{uz2}^{\mathrm{T}} & \mathbf{0} & 0 & K_{TMD2} \end{bmatrix} \tag{3c}$$

$$\mathbf{C} = \begin{bmatrix} \mathbf{C}_{ww} + \mathbf{C}_{wwT1} + \mathbf{C}_{wwT2} & \mathbf{C}_{wu} + \mathbf{C}_{wuT1} + \mathbf{C}_{wuT2} & \mathbf{0} & \mathbf{C}_{wz1} & \mathbf{C}_{wz2} \\ \mathbf{C}_{wu}^{\mathrm{T}} + \mathbf{C}_{wuT1}^{\mathrm{T}} + \mathbf{C}_{wuT2}^{\mathrm{T}} & \mathbf{C}_{uu} + \mathbf{C}_{uuT1} + \mathbf{C}_{uuT2} & \mathbf{0} & \mathbf{C}_{uz1} & \mathbf{C}_{uz2} \\ \mathbf{0} & \mathbf{0} & \mathbf{0} & \mathbf{0} & \mathbf{0} \\ \mathbf{C}_{wz1}^{\mathrm{T}} & \mathbf{C}_{uz1}^{\mathrm{T}} & \mathbf{0} & C_{TMD1} & 0 \\ \mathbf{C}_{wz2}^{\mathrm{T}} & \mathbf{C}_{uz2}^{\mathrm{T}} & \mathbf{0} & 0 & C_{TMD2} \end{bmatrix} \tag{3d}$$

$$\mathbf{F}(t) = \left\{ \sum_{element} \left[\int_{-1}^{1} \left(\mathbf{N}(\eta) f(\eta, t) \mathbf{J}_c(\eta) \right) \mathrm{d}\eta, \quad \mathbf{0}_u, \quad \mathbf{0}_\psi, \quad 0, \quad 0 \right] \right\}^{\mathrm{T}} \tag{3e}$$

where the expressions $\mathbf{0}_u$ and $\mathbf{0}_\psi$ in the equivalent nodal force vector $\mathbf{F}(t)$ represent the null vectors, with their size corresponding to the vectors $\mathbf{u}(t)$ and $\boldsymbol{\psi}(t)$, respectively. All the sub-matrices given in Equation (3) have been presented in the Appendix.

To seek the numerical stability, one could transfer the nodal displacement vector into a dimensionless one by utilizing

$$\mathbf{T} = \begin{bmatrix} L_e\mathbf{I}_w & \mathbf{0} & \mathbf{0} & \mathbf{0} & \mathbf{0} \\ \mathbf{0} & L_e\mathbf{I}_u & \mathbf{0} & \mathbf{0} & \mathbf{0} \\ \mathbf{0} & \mathbf{0} & \mathbf{I}_\psi & \mathbf{0} & \mathbf{0} \\ \mathbf{0} & \mathbf{0} & \mathbf{0} & L_e & 0 \\ \mathbf{0} & \mathbf{0} & \mathbf{0} & 0 & L_e \end{bmatrix} \tag{4}$$

where L_e is the curvilinear length between the two nodes for a curved beam element. $\mathbf{I}_w$, $\mathbf{I}_u$ and $\mathbf{I}_\psi$ are the identity matrices with sizes corresponding to the vectors $\mathbf{w}$, $\mathbf{u}$ and $\boldsymbol{\psi}$, respectively.

Thus, the nodal displacement vector $\mathbf{q}$ can be expressed in the form of $\mathbf{q} = \mathbf{T}\mathbf{q}_d$, with $\mathbf{q}_d$ being a dimensionless vector. Hence, the equations of motion stated in Equation (2) can be transferred as

$$\mathbf{M}_d\ddot{\mathbf{q}}_d(t) + \mathbf{C}_d\dot{\mathbf{q}}_d(t) + \mathbf{K}_d\mathbf{q}_d(t) = \mathbf{F}_d(t) \tag{5}$$

where

$$\mathbf{M}_d = \mathbf{T}^{\mathrm{T}}\mathbf{M}\mathbf{T}, \quad \mathbf{C}_d = \mathbf{T}^{\mathrm{T}}\mathbf{C}\mathbf{T}, \quad \mathbf{K}_d = \mathbf{T}^{\mathrm{T}}\mathbf{K}\mathbf{T} \text{ and}$$
$$\mathbf{F}_d(t) = \mathbf{T}^{\mathrm{T}}\mathbf{F}(t)$$

It should be noted that the matrices $\mathbf{M}_d$, $\mathbf{C}_d$ and $\mathbf{K}_d$ are all related to the design variables S_{Ti}, K_{TMDi}, C_{TMDi} and M_{TMDi}.

3. Random vibration analysis

The state-space analysis method (Lutes and Sarkani, 2004) is utilized to evaluate the Power Spectral Density (PSD) and the Root Mean Square (RMS) of the response. The equations of motion, given in Equation (5), can be transformed to the state-space form as

$$\dot{\mathbf{z}}(t) + \mathbf{A}\mathbf{z}(t) = \mathbf{Q}(t) \tag{6}$$

where $\mathbf{z}$ is the state vector $\{\mathbf{q}_d, \dot{\mathbf{q}}_d\}^{\mathrm{T}}$, and

$$\mathbf{A} = \begin{bmatrix} \mathbf{0} & -\mathbf{I} \\ \mathbf{M}_d^{-1}\mathbf{K}_d & \mathbf{M}_d^{-1}\mathbf{C}_d \end{bmatrix} \text{ and } \mathbf{Q}(t) = \begin{Bmatrix} \mathbf{0} \\ \mathbf{M}_d^{-1}\mathbf{F}_d(t) \end{Bmatrix} \tag{7}$$

Knowing the PSD of the external excitation as $\mathbf{S}_{QQ}(\omega)$, then the PSD of the state-space vector can be expressed as

$$\mathbf{S}_{zz}(\omega) = [\mathrm{i}\omega\mathbf{I} + \mathbf{A}]^{-1}\mathbf{S}_{QQ}(\omega)\left([-\mathrm{i}\omega\mathbf{I} + \mathbf{A}]^{-1}\right)^{\mathrm{T}} \tag{8}$$

It is noted that for a stationary random process, the PSD of external excitation is a constant matrix, and thus $\mathbf{S}_{QQ}(\omega)$ can be simplified as $\mathbf{S}_0$. Hence, the state-space covariance matrix $\mathbf{C}_{zz}$ can be evaluated through

$$\mathbf{A}\mathbf{C}_{zz} + \mathbf{C}_{zz}\mathbf{A}^{\mathrm{T}} = 2\pi\mathbf{S}_0 \tag{9}$$

This is a Lyapunov equation and it must be noted that the diagonal part of matrix $\mathbf{C}_{zz}$ is the variance of every variables in the state vector $\mathbf{z}(t)$, and for the stationary random loading with a zero mean value, the RMS is basically the square root of the variance.

4. Optimization methods

In this section, the optimization problem will be clearly formulated and then the established hybrid optimization method will be presented.

4.1. Statement of the optimization problem

The objective is to find the optimum values of the location (S_{Ti}), damping coefficient (C_{TMDi}) and the stiffness (K_{TMDi}) of the attached TMD systems under a known mass (M_{TMDi}) and the number of the attached TMD systems, in order to minimize the response (RMS) of the deflection of the curved beam. In order to seek the numerical stability, the following dimensionless parameters are defined:

$$\mu_i = M_{TMDi}/M_s, \quad f_{TMD_i} = \omega_{TMDi}/\omega_n \text{ and}$$
$$\xi_{TMD}i = C_{TMDi}/2\sqrt{K_{TMDi}M_{TMDi}} \tag{10}$$

where ω_n and M_s are the nth natural frequency and mass of the structure without TMD, and $\omega_{TMDi} = \sqrt{(K_{TMDi}/M_{TMDi})}$ is the natural frequency of the ith attached TMD. The dimensionless variables μ_i, f_{TMDi} and ξ_{TMDi} are the mass ratio, frequency ratio and the damping factor of the ith attached TMD, respectively. The optimization problem for a given mass ratio (μ) subjected to random excitation can now be described as

$$\begin{aligned} &\text{Find the design variables} : \{X\} = \{\xi_{TMDi}, f_{TMDi}, S_{Ti}\} \\ &\text{To minimize} : \textit{RMS of Deflection} \\ &\text{Subjected to} : 0 \le \xi_{TMDi} \le 1, 0 \le f_{TMDi} \\ &\le 2.5, S_{Ti} \text{ along the beam.} \end{aligned} \tag{11}$$

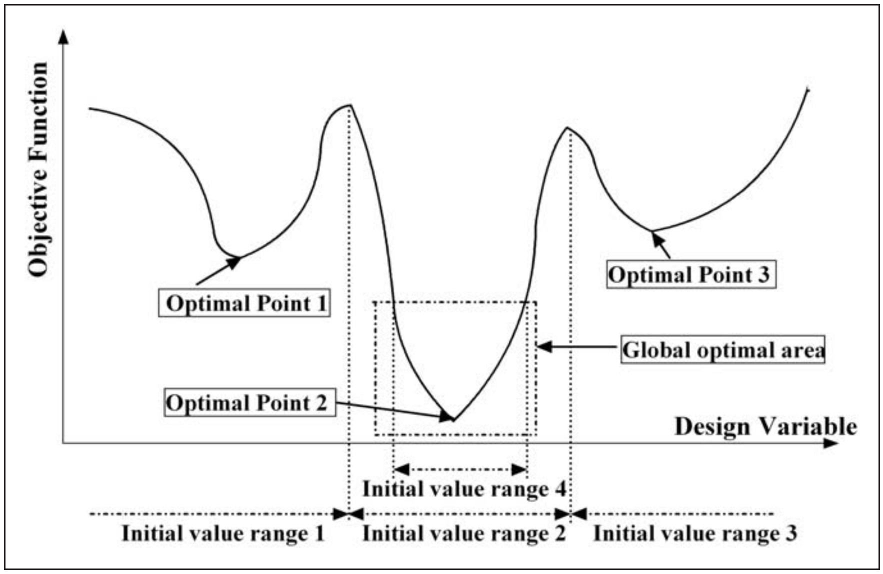

Figure 2. Schematic diagram of the hybrid optimization method for a global optimization problem.

Table 1. Definitions and programming methods for Genetic Algorithm optimization methodology

N_{var}	Number of design variable	N_{keep}	$N_{keep} = ceil\ (X_{rate} \times N_{pop})$
N_{pop}	Size of population	M_{rate}	Mutation rate
X_{rate}	Selection rate	N_{mute}	$ceil\ (M_{rate}(N_{pop}-1)N_{var})$
&	Convergence checking criterion (Cost_list (N_{keep})–Cost_list (1))/Cost_list (1) $\leq$ &)		

4.2. Hybrid optimization methodology

The optimization problem formulated in Equation (11) is based on the solution of a Lyapunov equation stated in Equation (9). Generally, it is a highly nonlinear optimization problem and may have many local optimums; in particular, the locations ($\boldsymbol{S_{Ti}}$) of the attached TMDs have been considered as one of the design variables in this study. To solve the established optimization problem, a hybrid optimization procedure has been developed, as illustrated in Figure 2, in which the curve represents the value of the cost function for a typical global optimization problem.

For the optimization problem illustrated in Figure 2, using a local optimization technique, such as the gradient-based optimizers, one may obtain "Optimal points 1, 2 and 3" based on the selected initial points located in the "Initial value ranges 1, 2 and 3", respectively. Obviously, only "Optimal point 2" is the global optimum point. The global optimizers, such as GA, may find the global optimum solution, but this is computationally expensive for some cases.

To circumvent those problems, the developed hybrid optimization procedure consists of two steps: (1) utilizing the GA to obtain the near-optimum value, which is illustrated in Figure 2 as the "Global optimal area"; (2) using the near-optimum point obtained in the last step as the initial point for the local optimization procedure (SQP).

The essential definitions and programming steps for the developed GA optimization method adopted in this study have been summarized in Table 1.

The term "ceil" in Table 1 represents rounding the variable to the nearest integer larger than or equal to it. The "Cost list" is the sorted newly generated population. In this study, the Rank Weighting Selection methodology (Haupt and Haupt, 2004) will be utilized to select the parents to generate the offspring; the selected mating methodology can be expressed as

$$\begin{aligned}\mathbf{Offspring}_1 &= \mathbf{M}a. - \boldsymbol{\beta}. \times (\mathbf{Ma}. - \mathbf{F}a);\\ \mathbf{Offspring}_2 &= \mathbf{M}a. + \boldsymbol{\beta}. \times (\mathbf{M}a. - \mathbf{F}a)\end{aligned} \tag{12}$$

where "$\mathbf{M}a$" and "$\mathbf{F}a$" represent one set of parent. $\boldsymbol{\beta}$ is a $1 \times N_{var}$ dimension vector, with the same dimension as "$\mathbf{M}a$" and "$\mathbf{F}a$", being generated randomly. The symbols ".–", ".+" and ".×" represent the element–element minus, plus and the product, respectively.

Table 2. Properties of the circular uniform beam

Elastic modulus	70 (GPa)	Shear coefficient	0.8438
Shear modulus	24.5 (GPa)	Beam radius	40 (m)
Area moment	0.01 (m^4)	Cross-sectional area	4 (m^2)
Density	2777 (kg/m^3)	Beam curve angle ()	40°

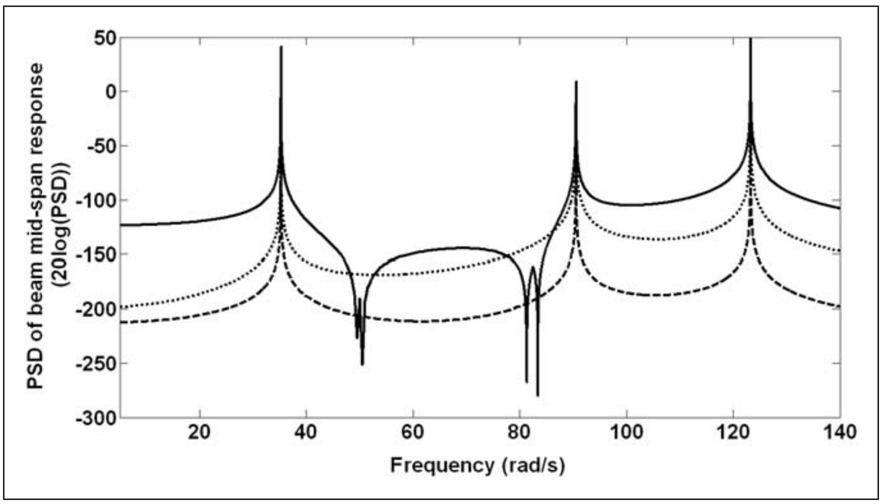

Figure 3. PSD of curved beam mid-span responses. Solid, dashed and dotted lines represent the transverse displacement (w), tangential displacement (u) and rotation (ψ), respectively.
PSD: Power Spectral Density.

5. Numerical examples

In this section, illustrative examples are presented to validate the design methodologies of the optimal MTMD system. The curved beam with a MTMD system has been illustrated in Figure 1 and its geometrical and material properties are listed in Table 2. In this study, the clamped–clamped boundary conditions have been considered, and the random load is in the form of a white noise, with the PSD of 10^{10} (N^2s/rad) applied uniformly and perpendicular to the beam central line.

5.1. Dynamic properties of the circular beam

The curved beam has been modeled using seven curved beam elements with four nodes per element (Yang et al., 2008). The first five natural frequencies of vibration for the curved beam are found to be as 19.4705, 35.2407, 64.4729, 90.5644 and 123.2884 (rad/s), respectively. The PSD of the curved beam's mid-span transverse displacement (w), tangential displacement (u) and rotation (ψ) responses under this random loading are illustrated in Figure 3.

It can be found from Figure 3 that in the low-frequency range (less than 140 (rad/s)), the structural responses mainly depend on the second, fourth and fifth vibration modes, and thus to obtain the best vibration suppression performance, the TMD systems should be optimally designed on the basis of these vibration modes.

Next, one could utilize the optimization methodology, established in Section 4, to catch the optimum point of MTMD systems step by step. Here, it is noted that in the following parts, the values related to the position of TMD system, shown in the following Tables and Figures, have been normalized with respect to the curvilinear length of the curved beam.

As mentioned before, one of the main purposes of this study is to establish an optimization procedure for the design of MTMDs. To seek a clear and simple expression, the illustrated example selected in this study is the symmetrical curved beam with the symmetrical boundary conditions, shown in Figure 1, and thus the TMD system should be also symmetrical.

Finally, it will be shown that the established methodology can easily be extended to the beams with any geometrical and boundary conditions.

Table 3. Optimal result for single tuned-mass-damper (TMD) design

Second vibration mode – Case (a) ($\mu = 0.01$)		Fourth vibration mode – Case (b) ($\mu = 0.02$)		Fifth vibration mode – Case (c) ($\mu = 0.015$)	
ξ_{TMD}	f_{TMD}	ξ_{TMD}	f_{TMD}	ξ_{TMD}	f_{TMD}
0.094	0.9512	0.0621	1.0235	0.1703	0.9647
0.093	0.9592	0.0589	1.0117	0.0923	0.9458

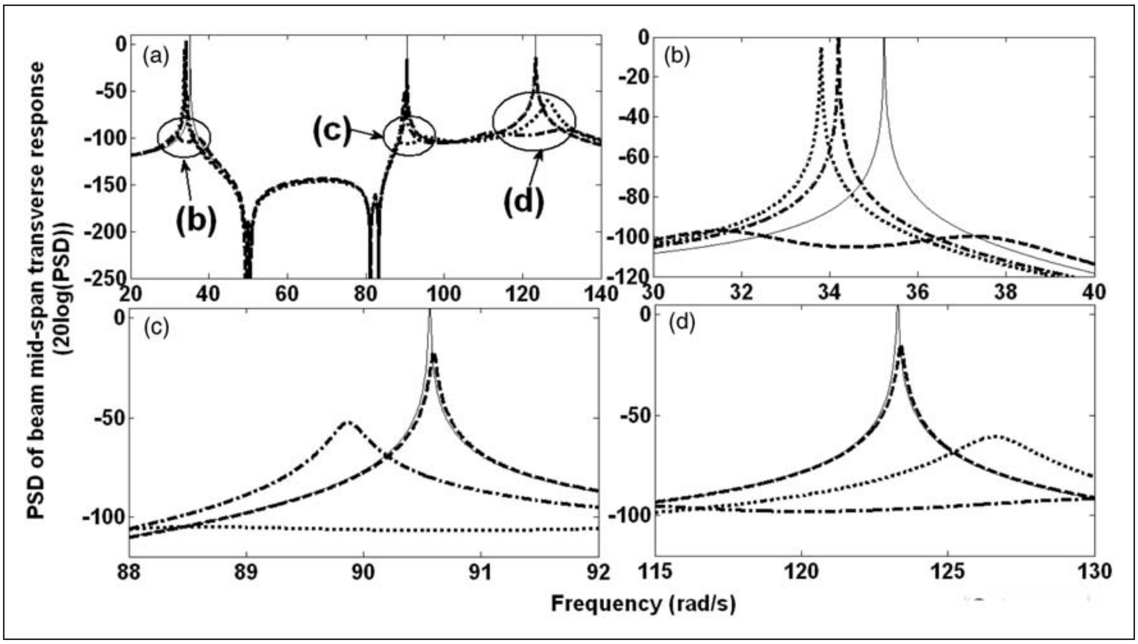

Figure 4. Beam mid-span transverse responses (w). (a) Frequency ranges 20–140 (rad/s); (b) Around second natural frequency; (c) around fourth natural frequency; (d) around fifth natural frequency. Solid, dashed, dotted and dashed-dotted lines represent uncontrolled structure, and structure with tuned-mass-damper Case (a), Case (b) and Case (c), listed in Table 3, respectively. PSD: Power Spectral Density.

5.2. Single TMD system

A single TMD system is attached onto the beam mid-span. Three different cases, listed in Table 3, were investigated. Cases (a), (b) and (c) are the designs based on the second, fourth and fifth vibration modes with different input mass ratio μ, respectively.

The optimization problem has been stated in Equation (11), and one could easily set the position variable as a constant value to find the optimum data. The mid-span transverse responses for the uncontrolled beam and the beam with the optimal single TMD designs, listed in Table 3, are illustrated in Figure 4. It can be seen that the effects of the optimally designed TMD for Cases (a), (b) and (c) are all restricted in their related tuned natural frequencies. Therefore, it is possible to design an optimal TMD for structures with multiple dominant vibration modes separately, and then combine them together to provide a MTMD design.

5.3. Distributed TMD design

In this section, the optimization procedure for the multiple TMDs system based on every vibration mode will be proposed. This type of multiple TMD system was named a distributed TMD (DTMD) system to make it distinct from the MTMD system based on multiple vibration modes, which will be discussed later. In the FE model, the design variable ($\boldsymbol{S_{Ti}}$) describing the position of the attached TMD includes one discrete variable representing the element that the TMD should be attached onto, and one continuous variable describing the coordinate of the TMD in that element. Therefore,

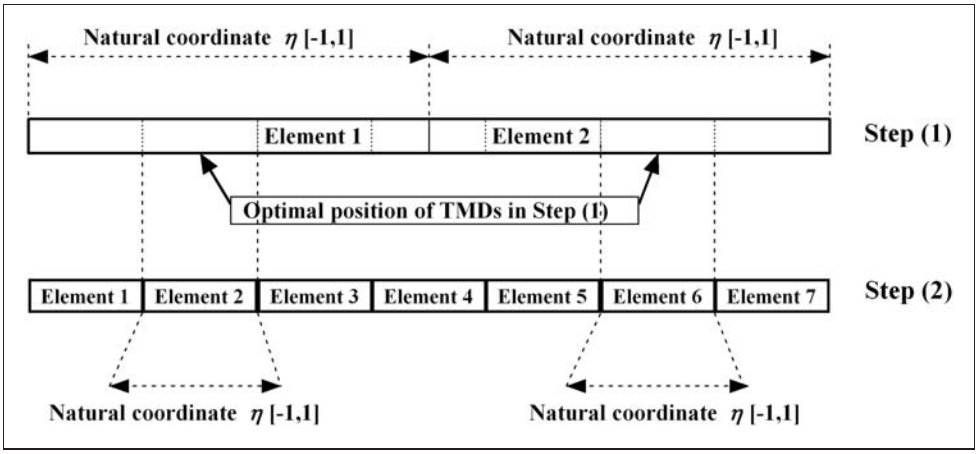

Figure 5. Diagram of the developed optimization procedures. TMD: tuned mass damper.

Table 4. Parameters of the Genetic Algorithm optimization

N_{pop}	8	X_{rate}	0.5	&	1×10^{-4}
N_{var}	3	M_{rate}	0.4		

Table 5. Optimal two symmetrical distributed tuned-mass-damper (DTMD) parameters based on the second vibration mode with mass ratio ($\mu = 0.005$) for each TMD

Design variables	ξ_{TMD}	f_{TMD}	Position_TMD1	Position_TMD2
	0.093	0.9592	0.5	0.5

the optimization procedure has been separated into two steps, as shown in Figure 5.

In Step (1) shown in Figure 5, the curved beam was modeled as two elements with 12 nodes per element (Yang et al., 2008); thus, the position of the attached TMD can simply be expressed by one continuous variable defined in the natural coordinate (η). Therefore, utilizing the optimum location obtained from Step (1), one could easily determine which elements of the TMD system should be located for the seven elements model employed in Step (2). The above procedure has been successfully implemented and most of the results listed in the following sections are taken as the final optimum data.

5.3.1. Two symmetrically attached DTMD systems. In this case three design variables (the frequency ratio, damping ratio and the attachment position) will be required for the optimization problem defined in Equation (11). The parameters used in the GA optimization have all been explained in Table 4.

5.3.1.1 Design based on the second vibration mode. Table 5 compares the optimum parameters for the two symmetrical DTMD designs, based on the second vibration mode for the optimization Step (2) shown in Figure 5. The mass ratio, μ, is assumed to be 0.005 for every attached TMD and thus the total mass ratio will be 0.01.

It can be seen from Table 5 that these two symmetrical DTMDs are attached exactly at the mid-span of the curved beam. Moreover, comparing the optimal TMD parameters with those listed in Table 3 for the second vibration mode with the mass ratio ($\mu = 0.01$), one can also find that they are identical. From these results one can easily conclude that the proposed hybrid optimization methodology has successfully caught the optimum points, and in particular the optimal location of the TMD system.

5.3.1.2 Design based on the fourth vibration mode. In this case, the mass ratio (μ) for every attached TMD is assumed to be 0.01. Table 6 compares the optimum results based on the GA, hybrid optimization and

Table 6. Optimal two symmetrical distributed tuned-mass-damper (DTMD) parameters based on the fourth vibration mode with mass ratio ($\mu = 0.01$) for each TMD – optimization Step (1)

Design variables	Optimal methodologies				
	GA	Hybrid	SQP_1	SQP_2	SQP_3
ξ_{TMD}	0.1783	0.1402	0.1403	0.1401	0.0681
f_{TMD}	0.9057	0.9278	0.9278	0.9256	1.0186
Position_TMD1	0.3045	0.3170	0.3170	0.3095	0.5
Position_TMD2	0.6955	0.6830	0.6830	0.6905	0.5
Objective ($\times 10^5$)	9.18428	9.0205	9.0205	9.0218	14.099

Note: SQP_1, SQP_2 and SQP_3 represent the Sequential Quadratic Programming (SQP) technique with initial values as {0.1, 1, −0.9}, {0.1, 1, 1} and the optimal value obtained from the Step (1) {0.0936, 0.9595, 0}, respectively.
GA: Genetic Algorithm.

Table 7. Optimal two symmetrical distributed tuned-mass-damper (DTMD) parameters based on the fourth vibration mode with mass ratio ($\mu = 0.01$) for each TMD – optimization Step (2)

Design variables	Optimal methodologies				
	GA	Hybrid	SQP_1	SQP_2	SQP_3
ξ_{TMD}	0.1409	0.1427	0.1427	0.1427	0.1427
f_{TMD}	0.9255	0.9238	0.9238	0.9238	0.9238
Position_TMD1	0.3054	0.3058	0.3058	0.3058	0.3058
Position_TMD2	0.6945	0.6942	0.6942	0.6942	0.6942
Objective ($\times 10^5$)	9.29139	9.29071	9.29071	9.29071	9.29071

Note: SQP_1, SQP_2 and SQP_3 represent the Sequential Quadratic Programming (SQP) technique with initial values as {0.1, 1, −0.9}, {0.1, 1, 1} and the optimal value obtained from the Step (1) {0.1403, 0.9278, −0.5616}, respectively.
GA: Genetic Algorithm.

SQP with different initial values for Step (1) of the optimization process.

Based on the optimal location for TMD1 (0.3170) and TMD2 (0.6830) being obtained in Step (1), it is found that the optimum elements for the seven-element model in Step (2) should be Elements 3 and 5, as illustrated in Figure 5. The optimum results for Step (2) are compared in Table 7.

Figure 6 compares the structural response around the fourth vibration mode for the curved beam with the optimal DTMD given in Table 7, and also with the optimal single TMD attached at the mid-span given in Table 3 for Case (b) having the mass ratio 0.02, which is equal to the total mass ratio in Table 7.

One can see from Figure 6 that the optimal two symmetrical DTMD systems developed in this section can provide much better vibration suppression effectiveness than that of the optimal single mid-span TMD under the same total mass ratio for the fourth mode. Comparing the results shown in Table 6, one can also find that: (1) utilizing different initial points, SQP would produce different local optimum data, which basically means that the proposed optimal problem is a typical global optimal case, and the local optimal methodology cannot guarantee the optimums; (2) the established GA methodology can catch the point close to the global optimum; and (3) the proposed hybrid methodology can not only catch the global optimums, but also is highly efficient.

5.3.1.3 Design based on the fifth vibration mode. The optimal two symmetrical DTMD systems tuned to the fifth vibration mode have been obtained as listed in Table 8. Through the response comparison, which will be shown later, it can be seen that the two symmetrical DTMD designs for the fifth mode can only improve the vibration suppression performance slightly, compared to the single mid-span TMD design. Therefore, it is necessary to investigate the case of three DTMDs for the fifth mode.

5.3.2. Three symmetrically attached DTMD systems. One could assume that three TMDs are attached to the curved beam in order to suppress the structural vibration due to the fifth vibration mode. Since the curved beam structure and boundaries are symmetrical in this

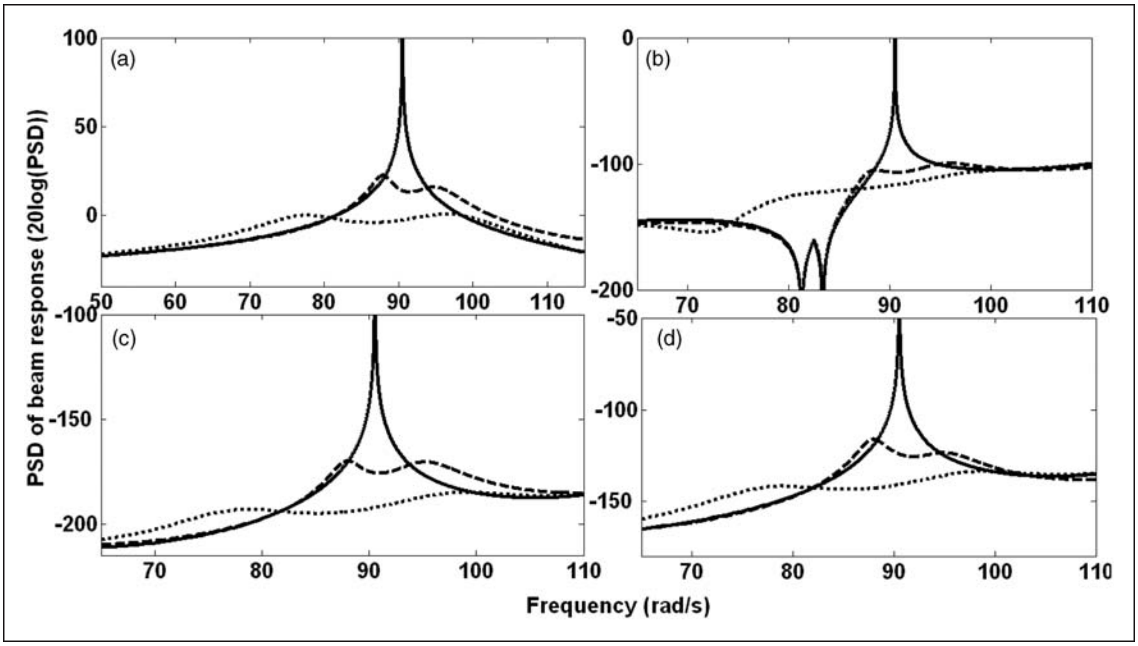

Figure 6. PSD of curved beam response comparison for different optimal tuned-mass-damper (TMD) designs based on the fourth vibration mode: (a) the fourth vibration modal response comparison; (b) curved beam mid-span's transverse response (*w*); (c) curved beam mid-span's tangential direction response (*u*); (d) curved beam mid-span's rotation response (ψ). Solid, dashed and dotted lines represent uncontrolled structure, structure with the optimal single mid-span TMD illustrated in Table 3 for Case (b), and that listed in Table 7, respectively.
PSD: Power Spectral Density.

example, it is clear that two of the three TMDs must be attached in symmetry and the third TMD is attached at the mid-span.

Let the mass ratio (μ) for every attached TMD be 0.005, and thus the total μ for these three attached TMDs is 0.015, which is the same as the optimal design stated in Tables 8 and 3 for Case (c). Considering the above discussion, the optimization problem in this section would have five design variables, as stated in Equation (13):

$$\begin{aligned}
\text{Find the design variables}: \{X\} &= \{\xi_{sTMD}, f_{sTMD}, \eta_{TMD}, \\
&\quad \xi_{TM}\mathrm{D}, f_{TMD}\} \\
\text{To minimize}: &\ \text{RMS of response for the} \\
&\ \text{5th vibration mode} \\
\text{Subjected to}: &\ -1 \le \eta_{TMD} \le, 0 \le \xi_{sTMD} \\
&\ \le 1, 0 \le f_{sTMD} \le 2.5, 0 \\
&\ \le \xi_{TM}\mathrm{D} \le 1, \text{ and } 0 \\
&\ \le f_{TMD} \le 2.5
\end{aligned} \tag{13}$$

where η_{TMD}, ξ_{sTMD}, f_{sTMD}, $\xi_{TM\mathrm{D}}$ and $f_{TM\mathrm{D}}$ represent the respective position, damping factor, and the frequency ratio of both the symmetrical and the mid-span TMDs. The required parameters for the GA optimization methodology have been defined in Table 9.

To illustrate the accuracy and convergence of the developed hybrid and GA optimization techniques in this section, the developed hybrid optimization technique has been repeated six times. The optimum results for each run obtained by the GA and hybrid optimization methods in Step (1) are provided in Table 10. The GA convergence analysis for every calculation listed in Table 10 is illustrated in Figure 7.

The term "position" in Table 10 represents the position of one of the symmetrically attached TMDs. The results show that the optimum locations will converge to two different points with close values of the objective function. Hence, one can realize that different optimum values of the design variables can provide close values of the objective function, which basically means that the optimization problem stated in Equation (13) is a very complex problem, having multiple local optimum points with a close value of objective function. Furthermore, the developed GA and hybrid techniques are capable of catching all those points. It should be mentioned that the convenience analysis has also been conducted for each set of either TMD or the DTMD design presented in this study, and perfect convergence

Table 8. Optimal two symmetrical distributed tuned-mass-damper (DTMD) parameters based on the fifth vibration mode with mass ratio ($\mu = 0.0075$) for each TMD

Design variables	ξ_{TMD}	f_{TMD}	Position_TMD1	Position_TMD2
	0.0953	0.9634	0.1715	0.8285

Table 9. Parameters of the Genetic Algorithm optimization

N_{pop}	12	X_{rate}	0.5	&	1×10^{-4}
N_{var}	5	M_{rate}	0.2		

Table 10. Optimal three tuned mass dampers (TMDs) based on the fifth vibration mode with mass ratio ($\mu = 0.005$) for each TMD – optimization Step (1)

Times	Optimal method	Design variables					Objective function ($\times 10^6$)
		ξ_{sTMD}	f_{sTMD}	Position	ξ_{TMD}	f_{TMD}	
1	GA	0.0833	0.9362	0.1760	0.5418	2.48	2.1556
	Hybrid	0.0767	0.9814	0.1915	0.5	2.5	2.0240
2	GA	0.0984	0.9825	0.1854	0.4372	1.2716	2.0485
	Hybrid	0.0782	0.9780	0.1823	0.0001	1.128	2.0272
3	GA	0.1284	0.8902	0.1770	0.6436	1.0543	2.4564
	Hybrid	0.0782	0.9781	0.1823	0.8115	2.42	2.0272
4	GA	0.0906	0.9429	0.1765	0.7063	1.2192	2.1176
	Hybrid	0.0782	0.9781	0.1821	1	2.2892	2.0272
5	GA	0.1370	0.9255	0.4999	0.0309	2.5	2.2298
	Hybrid	0.081	0.9647	0.5	0.9985	2.48	2.044
6	GA	0.1655	0.9118	0.4870	0.2687	1.3450	2.3849
	Hybrid	0.081	0.9647	0.5	0.0001	1.125	2.0436

GA: Genetic Algorithm.

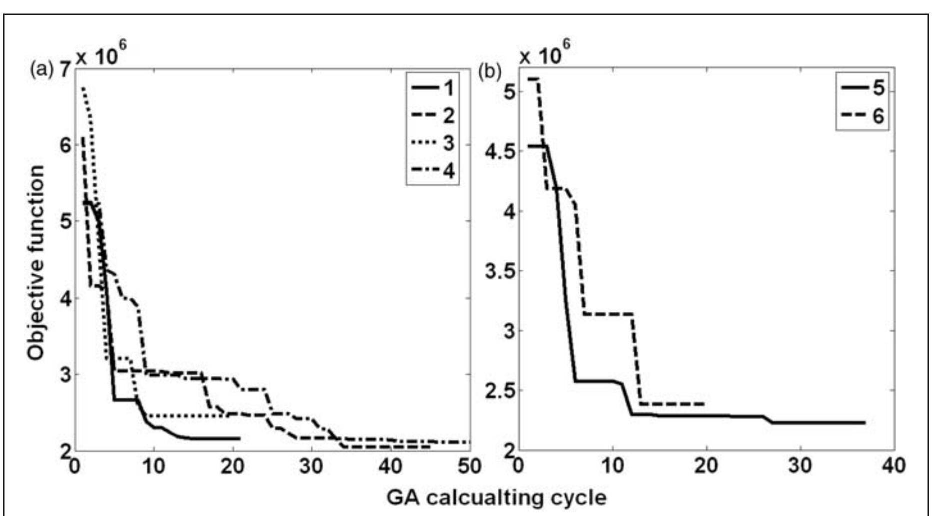

Figure 7. Generic Algorithm (GA) convergence analysis for each calculation as stated in Table 10: (a) for the first through fourth calculations; (b) for the fifth and sixth calculations.

Table 11. Optimal three tuned mass dampers (TMDs) based on the fifth vibration mode with mass ratio ($\mu = 0.005$) for each TMD – optimization Step (2)

Optimal method	Design variables					Objective function ($\times 10^6$)
	ξ_{sTMD}	f_{sTMD}	Position	ξ_{TMD}	f_{TMD}	
Hybrid	0.0637	1.0245	0.1862	0.0525	0.9034	1.8076

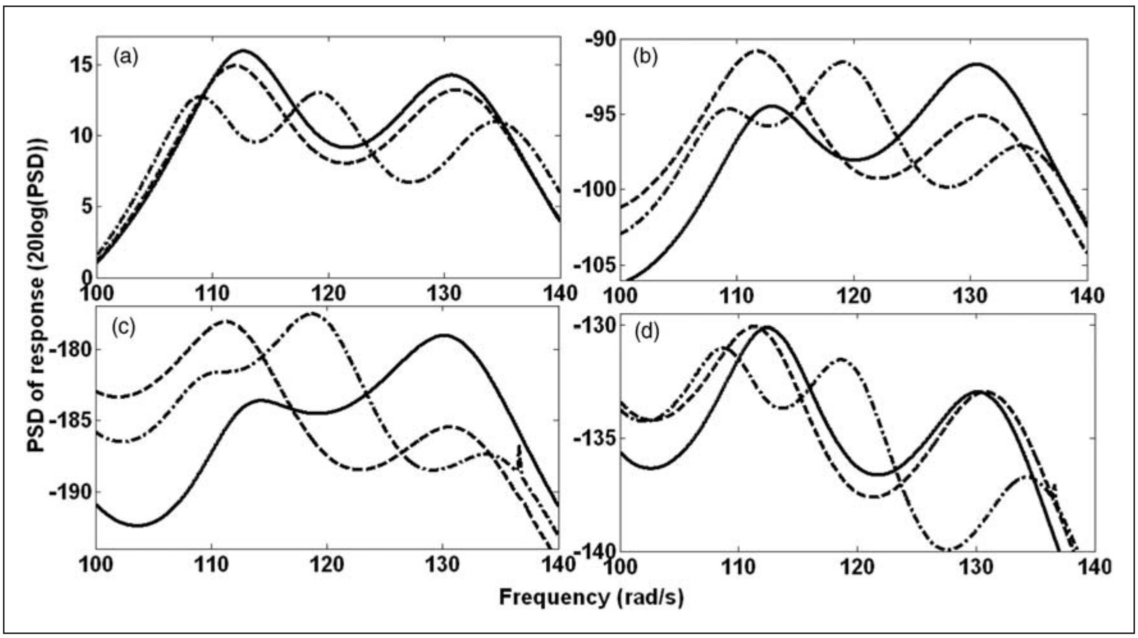

Figure 8. PSD of structural mid-span response around the fifth vibration mode: (a) the fifth vibration modal response; (b) the transverse response (w); (c) the tangential direction (u) response; (d) the rotation (ψ) response. Solid, dashed, and dashed-dotted lines represent structures with different optimal tuned-mass-damper design methods, Table 3 for Case (c), Table 8, and Table 11, respectively, based on the fifth mode.
PSD: Power Spectral Density.

properties have been observed. Here, for the sake of clarity, the analysis for the case of three DTMD designs, based on the fifth mode, has been developed.

As mentioned before, the main purpose of Step (1), shown in Figure 5, is to catch the optimum elements for the seven-element beam model in Step (2). Although the optimum damping factor and frequency ratio, particularly for the mid-span TMD, are significantly different in the first to fourth calculations, the optimum locations for the symmetrically attached TMDs are all located in elements 2 and 6 for the seven-element model in Step (2). The optimum design data for Step (2) is listed in Table 11.

Figure 8 compares the structural response for three different optimum TMD designs, based on the fifth vibration mode, which are one mid-span TMD (Table 3 for Case (c)), two symmetrical DTMDs (Table 8) and three DTMDs (Table 11). It should be noted that these three optimum TMD designs are all based on the same input of total mass ratio (μ).

One could easily find from Figure 8 that the optimum three DTMD systems listed in Table 11 provide the best vibration suppression for the fifth mode with respect to those of the single and two symmetrical TMD systems.

5.4. Tuned mass damper design based on antinodes

In this section, the traditional antinodes TMD design is applied to the curved beam, in particular for the fourth and fifth modes. Figure 9 illustrates the second, fourth and fifth vibration modal shapes of the curved beam. Since the TMD will be attached at the antinodes, the design will be focused on the values of damping and stiffness. Therefore, one can still utilize the

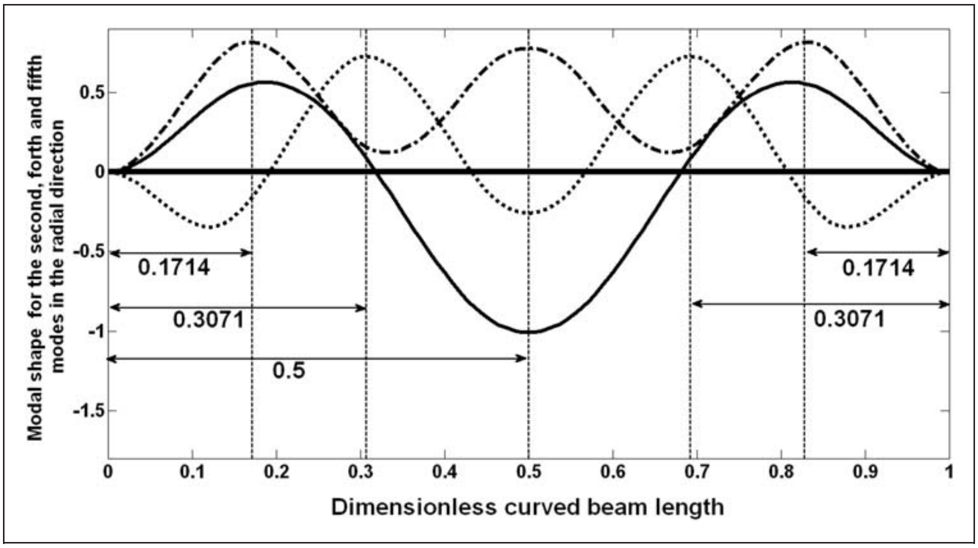

Figure 9. Modal shapes for beam transverse response (*w*). Solid, dotted and dashed-dotted lines represent the modal shape for second, fourth and fifth modes, respectively.

Table 12. Optimal tuned-mass-damper design comparison

Design mode		Design variables					Objective function ($\times 10^6$)
		ξ_{TMD}		f_{TMD}		Position	
Fourth mode	Table 7	0.1427		0.9238		0.3058	0.92907
	antinodes	0.143		0.9241		0.3071	0.92912
Fifth mode		Symmetry	Mid-span	Symmetry	Mid-span		
	Table 11	0.0637	0.0525	1.0245	0.9034	0.1862	1.8076
	antinodes	0.0712	0.051	1.0156	0.8976	0.1714	1.8146

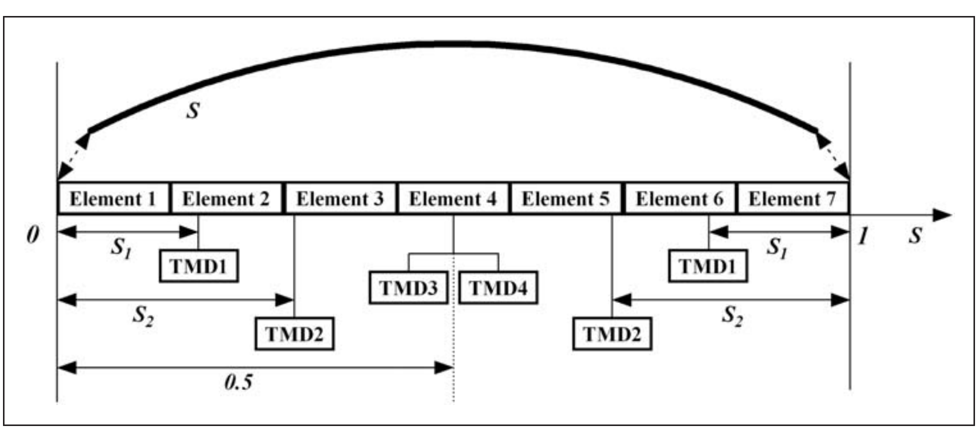

Figure 10. Optimal multiple tuned-mass-damper (MTMD) design.

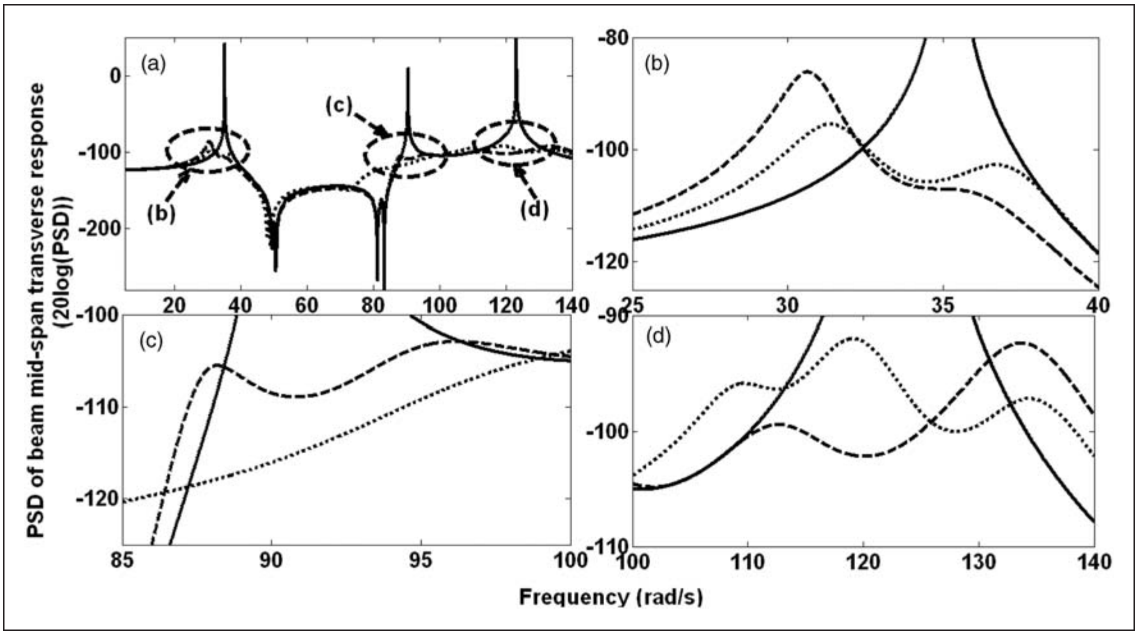

Figure 11. PSD of curved beam mid-span transverse response (w) comparison: (a) frequency ranges 5–140 (rad/s); (b) around second natural frequency; (c) around fourth natural frequency; (d) around fifth natural frequency. Solid, dashed and dotted lines represent uncontrolled structure, structure with optimal multiple tuned mass damper for Strategies 1 and 2, respectively.
PSD: Power Spectral Density.

Table 13. Optimal multiple tuned-mass-damper (MTMD) design strategies. Strategy 1: three attached MTMDs in the curved beam mid-span; Strategy 2: six attached MTMDs

Optimal strategies	Optimal parameters	Vibration modes		
Strategy 1 (Total mass ratio (μ) 4.5%)		Second mode Table 3 Case (a)	Fourth mode Table 3 Case (b)	Fifth mode Table 3 Case (c)
	Number of TMDs	1	1	1
	Mass ratio	0.01	0.02	0.015
	(Mid-span) ξ_{TMD}	0.093	0.0598	0.0923
	(Mid-span) f_{TMD}	0.9592	1.0117	0.9458
Strategy 2 (Total mass ratio (μ) 4.5%)		Second mode Table 3 Case (a)	Fourth mode Table 7	Fifth mode Table 11
	Number of TMDs	1	2	3
	Mass ratio	0.01	0.01	0.005
	(Mid-span) ξ_{TMD}	0.093		0.0525
	(Mid-span) f_{TMD}	0.9592		0.9034
	Position	Mid-span	$S_2 = 0.3058$	$S_1 = 0.1862$
	(Symmetry) ξ_{TMD}		0.1427	0.0637
	(Symmetry) f_{TMD}		0.9238	1.0245

Note: Parameters S_1 and S_2 are defined in Figure 10.

optimization problem listed in Equation (11) with the known TMD position to obtain the optimal antinodes TMD design.

Table 12 compares the antinodes TMD designs with those listed in Tables 7 and 11 for the designs based on the fourth and fifth modes. From the results shown in Table 12, one could easily find that (a) the traditional antinodes TMD design can provide a better vibration suppression performance to those listed in Tables 7 and 11; (b) although the values of the objection function for the two DMTD designs based on the fifth mode are close together, the attachment position has around 8% deviation.

In examining Figure 9, one could shed some light on some phenomenon shown in Section 5.3: (1) the two symmetrical TMD designs, based on the second mode, are exactly attached to the mid-span and the optimum data are identical to those obtained for the single mid-span TMD, as shown in Section 5.2; (2) the two symmetrical TMD designs, based on the fourth mode, can provide superior vibration suppression performance when compared to that of a single mid-span design; (3) the three TMD designs, based on the fifth mode, can provide the best performance; (4) one possible optimum location for the optimal design, based on the fifth mode, is to attach all the TMDs to the mid-span. From the above observations, it can be concluded that the fundamental issue for the TMD design of continuous structures is both the modal shape and the optimal location of the TMD system being close to the relative antinode(s).

5.5. Design based on multiple vibration modes

The vibration suppression of a curved beam using the TMD technology, based on the second, fourth and fifth vibration modes, has been separately investigated. The validity of every optimal TMD or DTMD design has been verified through the response comparisons. Based on the results discussed above, one may combine these optimal TMD systems to establish an optimal MTMD system, as shown in Figure 10, to suppress all the three modes simultaneously.

The term "TMD3" in Figure 10 is the optimal single mid-span TMD, based on the second mode, as Case (a) listed in Table 3. The term "TMD2" is the optimal two symmetrical DTMDs based on the fourth mode listed in Table 7. The terms "TMD1" and "TMD4" are the optimal three DTMDs based on the fifth mode listed in Table 11.

In order to verify the validity of the proposed optimal MTMD schematic, shown in Figure 11, two sets of optimal MTMD designs, listed in Table 13, were investigated. It should be noted from Table 13 that, for these two strategies, the total mass ratio of the TMD systems for every vibration mode and also for the complete TMD system are the same. The mid-span beam transverse responses w for both the uncontrolled structure and the structure with the attached optimal MTMD designs are illustrated in Figure 11.

It can be concluded from the results shown in Figure 11 that Strategy 2, presented in Table 13, is the best MTMD design, which provides the superior vibration suppression performance for the response around the second, fourth and fifth vibration modes. Furthermore, it has the smallest effect on the original structural dynamic properties, and thus on the performance of the original TMD design focusing on every vibration mode.

6. Conclusion

This study presents a thorough investigation on the vibration suppression of continuous systems in the form of a curved beam-type structure, subjected to random loadings, using the MTMD system. The FE formulation for the curved beam with the attached MTMD has been successfully derived. The developed FE methodology presents a comprehensive approach, and one can easily extend the general study to many structures with different boundary conditions and various geometrical and mechanical properties.

A hybrid optimization methodology that combines the global optimization method, based on a GA, and the local optimizer, based on SQP, has also been established. It has then been combined with the previously derived FE analysis module to find the optimal values of the design parameters, namely, the viscous damping coefficient, the spring stiffness and the attachment position of the TMD system.

Although the illustrated examples presented in this study are for the symmetrical beams with symmetrical boundary conditions, the modeling with the analysis and the optimization procedures can easily be extended to various beams with different boundary conditions. Basically, this research work presents an optimal design procedure for the MTMD system attached to a main structure having multiple dominant vibration modes and/or antinodes.

Funding

This work was supported by the Natural Sciences and Engineering Research Council of Canada (NSERC) and the Fundamental Research Funds for Central Universities, SCUT (No: 2012ZZ0109).

References

Chen TH and Huang YH (2004) Timoshenko beam with tuned mass dampers and its design curves. *Journal of Sound and Vibration* 278(4–5): 873–888.

Den Hartog JP (1956) *Mechanical Vibrations*, 4th ed. New York: McGraw Hill.

Esmailzadeh E and Jalili N (1998) Optimum design of vibration absorbers for structurally damped Timoshenko beams. *Journal of Vibration and Acoustics* 120(4): 833–841.

Fitzpatrick T, Dallard P, Bourva SL, et al (2001) *Linking London: The Millennium Bridge*. London: The Royal Academy of Engineering.

Haupt RL and Haupt SE (2004) *Practical Genetic Algorithms*, 2nd ed. Hoboken, NJ: John Wiley & Sons Inc.

Igusa T and Xu T (1994) Vibration control using multiple tuned mass dampers. *Journal of Sound and Vibration* 175(4): 491–503.

Lutes LD and Sarkani S (2004) *Random Vibration: Analysis of Structural and Mechanical Systems*. Boston, MA: Elsevier.

Manikanahally DN and Crocker MJ (1991) Vibration absorbers for hysterestically damped mass-loaded beams. *Journal of Vibration and Acoustics* 113(1): 116–122.

Rana R and Soong TT (1998) Parametric study and simplified design of tuned mass dampers. *Engineering Structures* 20(3): 193–204.

Rao SR (1996) *Engineering Optimization: Theory and Practice*. New York: John Wiley & Sons.

Rice HJ (1993) Design of multiple vibration absorber systems using modal data. *Journal of Sound and Vibration* 160(2): 378–385.

Rüdinger F (2006) Tuned mass damper with fractional derivative damping. *Journal of Engineering Structures* 28(13): 1774–1779.

Yang F, Sedaghati R and Esmailzadeh E (2008) Free in-plane vibration of general curved beams using finite element method. *Journal of Sound and Vibration* 318(4–5): 850–867.

Yang F, Sedaghati R and Esmailzadeh E (2009) Vibration suppression of non-uniform curved beam under random loading using optimal tuned mass damper. *Journal of Vibration and Control* 15(2): 233–261.

Yang F, Sedaghati R and Esmailzadeh E (2010) Optimal vibration suppression of Timoshenko beam with tuned-mass-damper using finite element method. *Journal of Vibration and Acoustics* 131(3): 031006–8.

Younesian D, Esmailzadeh E and Sedaghati R (2006) Passive control of vibration of beams subject to random excitations with peaked PSD. *Journal of Vibration and Control* 12(9): 941–953.

Appendix: sub-matrices in Equation (3)

$$\mathbf{M}_{ww} = \sum_{element}\left\{\int_{-1}^{1}\left[\gamma\mathbf{N}(\eta)^{\mathrm{T}}\mathbf{A}_a(\eta)\mathbf{N}(\eta)\mathbf{J}_c(\eta)\right]\mathrm{d}\eta\right\} \quad (A.1)$$

$$\mathbf{M}_{uu} = \sum_{element}\left\{\int_{-1}^{1}\left[\gamma\mathbf{N}(\eta)^{\mathrm{T}}\mathbf{A}_a(\eta)\mathbf{N}(\eta)\mathbf{J}_c(\eta)\right]\mathrm{d}\eta\right\} \quad (A.2)$$

$$\mathbf{M}_{\psi\psi} = \sum_{element}\left\{\int_{-1}^{1}\left[\gamma\mathbf{N}(\eta)^{\mathrm{T}}\mathbf{I}(\eta)\mathbf{N}(\eta)\mathbf{J}_c(\eta)\right]\mathrm{d}\eta\right\} \quad (A.3)$$

$$\mathbf{K}_{ww} = \sum_{element}\left\{\int_{-1}^{1}\left[[k_q G\mathbf{A}_a(\eta)\mathbf{B}(\eta)^{\mathrm{T}}\mathbf{B}(\eta)\mathbf{J}_c^{-1}(\eta) + \frac{E\mathbf{A}_a(\eta)}{\rho(\eta)^2}\mathbf{N}(\eta)^{\mathrm{T}}\mathbf{N}(\eta)\mathbf{J}_c(\eta)\right]\mathrm{d}\eta\right\} \quad (A.4)$$

$$\mathbf{K}_{wu} = \sum_{element}\left\{\int_{-1}^{1}\left[\frac{E\mathbf{A}_a(\eta)}{\rho(\eta)}\mathbf{N}(\eta)^{\mathrm{T}}\mathbf{B}(\eta) - \frac{k_q G\mathbf{A}_a(\eta)}{\rho(\eta)}\mathbf{B}(\eta)^{\mathrm{T}}\mathbf{N}(\eta)\right]\mathrm{d}\eta\right\} \quad (A.5)$$

$$\mathbf{K}_{w\psi} = \sum_{element}\left\{-\int_{-1}^{1}\left[k_q G\mathbf{A}_a(\eta)\mathbf{B}(\eta)^{\mathrm{T}}\mathbf{N}(\eta)\right]\mathrm{d}\eta\right\} \quad (A.6)$$

$$\mathbf{K}_{uu} = \sum_{element}\left\{\int_{-1}^{1}\left[E\mathbf{A}_a(\eta)\mathbf{B}(\eta)^{\mathrm{T}}\mathbf{B}(\eta)\mathbf{J}_c^{-1}(\eta) + \frac{k_q G\mathbf{A}_a(\eta)}{\rho(\eta)^2}\mathbf{N}(\eta)^{\mathrm{T}}\mathbf{N}(\eta)\mathbf{J}_c(\eta)\right]\mathrm{d}\eta\right\} \quad (A.7)$$

$$\mathbf{K}_{u\psi} = \sum_{element}\left\{\int_{-1}^{1}\left[\frac{k_q G\mathbf{A}_a(\eta)}{\rho(\eta)}\mathbf{N}(\eta)^{\mathrm{T}}\mathbf{N}(\eta)\mathbf{J}_c(\eta)\right]\mathrm{d}\eta\right\} \quad (A.8)$$

$$\mathbf{K}_{\psi\psi} = \sum_{element}\left\{\int_{-1}^{1}\left[E\mathbf{I}(\eta)\mathbf{B}(\eta)^{\mathrm{T}}\mathbf{B}(\eta)\mathbf{J}_c^{-1}(\eta) + k_q G\mathbf{A}_a(\eta)\mathbf{N}(\eta)^{\mathrm{T}}\mathbf{N}(\eta)\mathbf{J}_c(\eta)\right]\mathrm{d}\eta\right\} \quad (A.9)$$

$$\mathbf{K}_{wwTi} = \left[\mathbf{N}(\eta)^{\mathrm{T}}\mathbf{N}(\eta)K_{TMD}\cos^2(\alpha(\eta))\right]_{\eta=\eta_{TMDi}} \quad (A.10)$$

$$\mathbf{K}_{wuTi} = \left[\mathbf{N}(\eta)^{\mathrm{T}}\mathbf{N}(\eta)K_{TMD}\cos(\alpha(\eta))\sin(\alpha(\eta))\right]_{\eta=\eta_{TMDi}} \quad (A.11)$$

$$\mathbf{K}_{uuTi} = \left[\mathbf{N}(\eta)^{\mathrm{T}}\mathbf{N}(\eta)K_{TMD}\sin^2(\alpha(\eta))\right]_{\eta=\eta_{TMDi}} \quad (A.12)$$

$$\mathbf{K}_{uzi} = -\left[\mathbf{N}(\eta)^{\mathrm{T}}K_{TMD}\sin(\alpha(\eta))\right]_{\eta=\eta_{TMDi}} \quad (A.13)$$

$$\mathbf{K}_{wzi} = -\left[\mathbf{N}(\eta)^{\mathrm{T}}K_{TMD}\cos(\alpha(\eta))\right]_{\eta=\eta_{TMDi}} \quad (A.14)$$

$$\mathbf{C}_{ww} = \sum_{element}\int_{-1}^{1} C_w\mathbf{N}(\eta)^{\mathrm{T}}\mathbf{N}(\eta)\mathbf{J}_c(\eta)\mathrm{d}\eta \quad (A.15)$$

$$\mathbf{C}_{uu} = \sum_{element}\int_{-1}^{1} C_u\mathbf{N}(\eta)^{\mathrm{T}}\mathbf{N}(\eta)\mathbf{J}_c(\eta)\mathrm{d}\eta \quad (A.16)$$

$$\mathbf{C}_{wwTi} = \left[\mathbf{N}(\eta)^{\mathrm{T}}\mathbf{N}(\eta)C_{TMD}\cos^2(\alpha(\eta))\right]_{\eta=\eta_{TMDi}} \quad (A.17)$$

$$\mathbf{C}_{wuTi} = \left[\mathbf{N}(\eta)^{\mathrm{T}}\mathbf{N}(\eta)C_{TMD}\cos(\alpha(\eta))\sin(\alpha(\eta))\right]_{\eta=\eta_{TMDi}} \quad (A.18)$$

$$\mathbf{C}_{uuTi} = \left[\mathbf{N}(\eta)^{\mathrm{T}}\mathbf{N}(\eta)C_{TMD}\sin^2(\alpha(\eta))\right]_{\eta=\eta_{TMDi}} \quad \text{(A.19)}$$

$$\mathbf{C}_{uzi} = -\left[\mathbf{N}(\eta)^{\mathrm{T}}C_{TMD}\sin(\alpha(\eta))\right]_{\eta=\eta_{TMDi}} \quad \text{(A.20)}$$

$$\mathbf{C}_{wzi} = -\left[\mathbf{N}(\eta)^{\mathrm{T}}C_{TMD}\cos(\alpha(\eta))\right]_{\eta=\eta_{TMDi}} \quad \text{(A.21)}$$

where $[B(\eta)] = d[N(\eta)]/d\eta$.

The Jacobian $\mathbf{J}_c(\eta)$can be evaluated through

$$\mathbf{J}_c(\eta) = \frac{ds}{\mathrm{d}\eta} = \sqrt{\left(\frac{dx}{\mathrm{d}\eta}\right)^2 + \left(\frac{dy}{\mathrm{d}\eta}\right)^2} = \sqrt{(\mathbf{B}(\eta)\mathbf{x})^2 + (\mathbf{B}(\eta)\mathbf{y})^2} \quad \text{(A.22)}$$

and the radius $\rho(\eta)$ can be evaluated through the following equation:

$$\frac{1}{\rho} = \frac{d^2y/dx^2}{\{1 + (dy/dx)^2\}^{1.5}} \quad \text{(A.23)}$$

and the parameters $\cos(\alpha(\eta))$ and $\cos(\alpha(\eta))$ can be evaluated through

$$\cos(\alpha(\eta_{TMDi})) = \mathbf{B}(\eta_{TMDi})\mathbf{x}/\mathbf{J}_c(\eta_{TMDi}) \quad \text{(A.24)}$$

$$\sin(\alpha(\eta_{TMDi})) = \mathbf{B}(\eta_{TMDi})\mathbf{y}/\mathbf{J}_c(\eta_{TMDi}) \quad \text{(A.25)}$$